Hindawi
Complexity
Volume 2020, Article ID 9130875, 14 pages
https://doi.org/10.1155/2020/9130875

WILEY | Hindawi

Research Article

Fractional-Order Iterative Learning Control with Initial State Learning for a Class of Multiagent Systems

Xungen Li,[1,2] Shuaishuai Lv,[1,2] Mian Pan,[1] Qi Ma,[1] and Wenyu Cai[1]

[1]*The College of Electronics and Information, Hangzhou Dianzi University, Hangzhou 310018, China*
[2]*Pujiang Microelectronics and Intelligent Manufacturing Research Institute of Hangzhou Dianzi University, Jinhua 322200, China*

Correspondence should be addressed to Shuaishuai Lv; lvshuai@hdu.edu.cn

Received 11 June 2020; Revised 19 September 2020; Accepted 1 October 2020; Published 28 October 2020

Academic Editor: Oh-Min Kwon

To solve the consensus problem of fractional-order multiagent systems with nonzero initial states, both open- and closed-loop PD^{α}-type fractional-order iterative learning control are presented. Considering the nonzero states, an initial state learning mechanism is designed. The finite time convergences of the proposed methods are discussed in detail and strictly proved by using Lebesgue-p norm theory and fractional-order calculus. The convergence conditions of the proposed algorithms are presented. Finally, some simulations are applied to verify the effectiveness of the proposed methods.

1. Introduction

Fractional-order multiagent systems (FOMASs) is composed of multiple agents, which can coordinate with each other to perceive the external environment, and apply fractional-order calculus principle. Due to the autonomy, fault tolerance, flexibility, scalability, and collaboration capabilities of the FOMASs, it can be applied to the intelligent environment perception and intelligent operation, such as air formation control, traffic vehicle control, data convergence, sensor networks, and so on [1–4]. In order to realize the wide application of FOMASs, it is necessary to design the coordinated control effectively, including consensus control, formation control, coalescence control, and rendezvous control. And the consensus problem is the basic problem in FOMASs distributed coordination control. Its purpose is to design an appropriate distributed consensus control protocol based on the neighbor states of the agent and its own state information, so that the states of all the agents converge to the same value at a specific position or a certain moment.

The consensus problem of FOMASs was studied in [5] for the first time, in which the relationship between the consensus problem of FOMAS and the number of agents and fractional orders was discussed, and some control strategies were given to improve the convergence speed of the FOMASs. In the same year, Cao and Ren [6] also applied the consensus theory to the formation control problem of FOMASs. Since then, the research and application of FOMASs consensus problems have been emerging, including linear fractional-order multiagents [7–10] and nonlinear fractional-order multiagents [11–14]. Song and Cao [7] used the stability theory of FOSs and linear matrix inequality to study the consensus problem of linear FOMASs. And then they further considered the robust consensus problem of linear FOMASs when the fractional order satisfies $\alpha \in (0, 2)$[8]. Yu et al. [9] used the algebraic graph theory tool and the Lyapunov method to study the consensus problem of nonlinear FOMASs with a leader-following structure. Similarly, in [10, 11], the adaptive control and the sampling data control were designed to solve the consensus problem of nonlinear and linear FOMASs with and without leader-following structure, and some sufficient and necessary conditions related to fractional order, coupling gain, and Laplacian matrix spectrum were obtained to ensure that the system can achieve consensus. For the study of nonlinear FOMASs, there are also literatures [12–14].

However, most of the research just consider the asymptotic convergence problem of FOMASs, which means the tracking errors of the fractional-order agents gradually converge to zero as time increases. On some special occasions, such as industrial automatic production lines, the asymptotic convergence cannot meet the actual demands. As we all know, fractional-order iterative learning control (FOILC) methods for repetitive running systems can achieve complete tracking problems in finite time [15,16]. In [17,18], both distributed D^{α}- and PD^{α}-type FOILC were proposed and applied to linear FOMASs with fixed topology. Furthermore, for the linear time-varying integer-order system, Luo et al. proposed a FOILC framework with initial state learning and presented sufficient and necessary conditions for open-loop and closed-loop D^{α}-type FOILC. But for FOMASs, it has not been researched using open and closed FOILC.

In the literature [17], the consensus problem of FOMASs is discussed using FOLIC. However, the authors just considered the zero initial states of FOMASs, which must ensure the strict positioning of the initial state during the iteration process. In this paper, for linear time-varying FOMASs with fixing the initial states over the directed graph, we design several fractional iterative learning controllers with the initial states learning algorithms. The contributions are summarized as follows. First, considering the nonzero initial state of FOMASs, we propose three different forms of fractional-order iterative learning updating laws. Second, an initial state learning algorithm together with the FOILC updating laws is designed. Finally, the convergences of the proposed algorithm are discussed and the convergence conditions are presented. The theoretical analysis and simulation experiments verify the effectiveness of the proposed method. The results show that both the tracking errors and the nonzero initial states can tend to zero in finite time as the iterative number increases.

The remainder of this paper is organized as follows. Section 2 overviews the related theories related to this article, including the graph theory, the definition of fractional calculus, and the problem formulation. The algorithm design and analysis employing FOILC with initial learning are discussed in Section 3. Section 4 demonstrates the simulation results to verify the effectiveness of the proposed methods. And briefly, conclusions are presented in Section 5.

2. Preliminaries

In this part, first, we introduce some basic definitions, lemmas, and properties, which will be used in the following sections.

2.1. Graph Theory. Consider N multiagents with the same dynamic. The direct graph $\mathbb{G} = \{\mathbb{V}, \mathbb{E}, \mathbf{M}\}$ is used to describe the information transfer between multiagents, where $\mathbb{V} = \{v_1, \ldots, v_N\}$ is the node set, $\mathbb{E} \subseteq \mathbb{V} \times \mathbb{V}$ is the edge set, and $\mathbf{M} = (a_{ik})_{N\times N}$ is the adjacency matrix of the direct graph. $(k, i) \in \mathbb{E} \subseteq \mathbb{V} \times \mathbb{V}$ is a direct edge of the agents k and i. The set of neighbors of the ith agent is denoted by $\mathbb{N}_i = \{k \in \mathbb{V}: (k, i) \in \mathbb{E}\}$. The matrix element $a_{ik} > 0$ represents node k passing information to node i; otherwise, $a_{ik} = 0$. Here, the communication topology graph has no self-loop phenomenon, namely, $a_{i,i} = 0$. $\mathbf{D} = \mathrm{diag}\{d_i, i \in \mathbb{S}_N\}$ is defined as the degree matrix, where $d_i = \sum_{k=1}^{N} a_{i,k}$, and $\mathbf{L} = \mathbf{D} - \mathbf{M}$ is the Laplacian matrix of the direct graph.

2.2. The Norm. In this paper, the vector Euclidian norm and its induced matrix norm is defined as $\|\cdot\|$. $\mathbf{I}_m \in \mathbb{R}^{m\times m}$ is the identity matrix. $\mathbb{C}^m[0, T]$ is defined as a function set and the mth derivative of $\mathbb{C}^m[0, T]^{\wedge}$ # is continuous over a finite time interval $[0, T]$. $\mathbb{R}$ and $\mathbb{N}$ are the sets of real and natural numbers. $\mathbb{S}_N = \{0, 1, \ldots, N\}$. Denote the Kronecker product by $\otimes$, for some matrices $\mathbf{A}$,$\mathbf{B}$, $\mathbf{C}$, and $\mathbf{D}$, the following properties will be satisfied such that

$$k(\mathbf{A}\otimes\mathbf{B}) = k\mathbf{A}\otimes\mathbf{B} = \mathbf{A}\otimes k\mathbf{B}, \tag{1}$$

$$(\mathbf{A}+\mathbf{B})\otimes\mathbf{C} = \mathbf{A}\otimes\mathbf{C} + \mathbf{B}\otimes\mathbf{C}, \tag{2}$$

$$(\mathbf{A}\otimes\mathbf{B})(\mathbf{C}\otimes\mathbf{D}) = \mathbf{AC}\otimes\mathbf{BD}, \tag{3}$$

$$\|\mathbf{A}\otimes\mathbf{B}\| = \|\mathbf{A}\|\cdot\|\mathbf{B}\|. \tag{4}$$

Definition 1. Assuming the continuous vector function $\mathbf{f}$: $[0, T] \longrightarrow \mathbb{R}^{\mathrm{n}}\mathbf{f}(t) = [f^1(t), f^2(t), \ldots, f^n(t)]^{\mathrm{T}}$, the Lebesgue-p norm of $\mathbf{f}(t)$ is defined as

$$\|\mathbf{f}(t)\|_p = \left[\int_0^T \left(\max_{1\le i\le n}|f^i(t)|\right)^p \mathrm{d}t\right]^{(1/p)}, \quad 1 \le p < \infty. \tag{5}$$

Lemma 1 (see [19]). *Assuming the functions $\mathbf{g}(t) \in \mathbb{L}^q[0, T]$ and $\mathbf{h}(t) \in \mathbb{L}^p[0, T]$, then the convolution generalized Yong inequality of the functions $\mathbf{g}(t)$ and $\mathbf{h}(t)$ is*

$$\|(\mathbf{g} * \mathbf{h})(t)\|_r \le \|\mathbf{g}(t)\|_q \|\mathbf{h}(t)\|_p, \tag{6}$$

where $1 \le \mathrm{p}, \mathrm{q}, \mathrm{r} \le \infty$, $(1/r) = (1/p) + (1/q) - 1$, and $(\mathbf{g} * \mathbf{h})(t) = \int_0^t \mathbf{g}(t-\tau)\mathbf{h}(\tau)d\tau$ is the convolution integral of $\mathbf{g}(t)$ and $\mathbf{h}(t)$. In particular, if $r = p$, the inequality is converted to $\|(\mathbf{g} * \mathbf{h})(t)\|_p \le \|\mathbf{g}(t)\|_1 \|\mathbf{h}(t)\|_p$.

2.3. Fractional Calculus

Definition 2 (see [21]). The [21, 22] Riemann–Liouville fractional integrals of $f(t)$ with order $\alpha \in (0, 1)$ are defined as

$$\begin{aligned} {}_{t_0}D_t^{-\alpha} f(t) &= \frac{1}{\Gamma(\alpha)}\int_{t_0}^{t} (t-\tau)^{\alpha-1} f(\tau)\mathrm{d}\tau, \quad (t > t_0), \\ {}_{t}D_t^{-\alpha} f(t) &= \frac{1}{\Gamma(\alpha)}\int_{t}^{T} (\tau-t)^{\alpha-1} f(\tau)\mathrm{d}\tau, \quad (t < T), \end{aligned} \tag{7}$$

where $\Gamma(\cdot)$ is gamma function. The left- and right-sided Caputo derivatives are

$$
\begin{aligned}
{}_{t_0}^{C}D_t^{\alpha} f(t) &= {}_{t_0}D_t^{-([\alpha]-\alpha+1)}\left[\frac{\mathrm{d}^{[\alpha]+1}}{\mathrm{d}t^{[\alpha]+1}} f(t)\right], \quad (t > t_0),\\
{}_{t}^{C}D_T^{\alpha} f(t) &= {}_{t}D_T^{-([\alpha]-\alpha+1)}\left[\frac{\mathrm{d}^{[\alpha]+1}}{\mathrm{d}t^{[\alpha]+1}} f(t)\right], \quad (t < T),
\end{aligned}
\tag{8}
$$

where $\alpha \in \mathbf{R}^+$ and $[\alpha]$ means the integral part of α.

Lemma 2 (see [20]). *Suppose the functions $f(t), g(t)$ are continuous in $[0,T]$, and ${}_{t}^{C}D_T^{\alpha} f(t)$, ${}_{0}^{C}D_T^{\alpha} g(t) (t \in [0,T])$ exist, then the fractional integration by parts is*

$$
\int_0^T \left({}_{t}^{C}D_T^{\alpha} f(t)\right) g(t)\mathrm{d}t = \int_0^T f(t)\left({}_{0}^{C}D_T^{\alpha} g(t)\right)\mathrm{d}t. \tag{9}
$$

Definition 3 (see [20, 23]). The Mittag–Leffler function can be described as

$$
E_{\alpha,\beta}(z) = \sum_{k=0}^{\infty} \frac{z^k}{\Gamma(\alpha k + \beta)} \quad (\alpha > 0, \beta > 0, z \in C^{n\times n}). \tag{10}
$$

Particularly, when $\beta = 1$, we can obtain

$$
E_{\alpha,1}(z) = E_{\alpha}(z) = \sum_{k=0}^{\infty} \frac{z^k}{\Gamma(\alpha k + 1)}, \quad (\alpha > 0, z \in C^{n\times n}). \tag{11}
$$

Lemma 3 (see [20]). *Let $\Phi_{\alpha,\beta}(A,t) = t^{\beta-1}E_{\alpha,\beta}(At^{\alpha}) t \in [0,+\infty) \alpha > 0$, $\beta > 0, z \in C^{n\times n}$; then we have*

$$
\begin{aligned}
&{}_{\tau}^{C}D_t^{1-\alpha} f(t)\boldsymbol{\Phi}_{\alpha,1}(A, t-\tau) = \boldsymbol{\Phi}_{\alpha,\alpha}(A, t-\tau), \quad 0 < \alpha < 1,\\
&\frac{\mathrm{d}}{\mathrm{d}\tau}\boldsymbol{\Phi}_{\alpha,1}(A, t-\tau) = -\boldsymbol{\Phi}_{\alpha,\alpha}(A, t-\tau)A, \quad \alpha > 0, A \in C^{n\times n}.
\end{aligned}
\tag{12}
$$

Lemma 4 (see [23]). *For the initial value problem*

$$
\begin{cases}
{}_{t_0}^{C}D_t^{\alpha} x(t) = \mathrm{A}x(t) + \mathrm{B}u(t),\\
x(t_0) = x_0.
\end{cases}
, \quad A \in C^{n\times n}, B \in C^{n\times p}, 0 < \alpha < 1. \tag{13}
$$

The Volterra-type nonlinear integral equation can be obtained as

$$
x(t) = \Phi_{\alpha,1}(A,t)x_0 + \int_{t_0}^{t} \Phi_{\alpha,\alpha}(A, t-\tau)\mathrm{B}u(\tau)\mathrm{d}\tau. \tag{14}
$$

Property 1. If $\mathbf{f}(t) \in \mathbb{C}(t_0, \infty)$, then $D^{1-\alpha}D^{\alpha}\mathbf{f}(t) = \mathbf{f}^{(1)}(t)$, $\alpha \in (0,1)$, where $f^{(1)}(t) = (\mathrm{d}/\mathrm{d}t)\mathbf{f}(t)$.

3. Problem Description

Considering N homogeneous fractional-order linear time-delay MASs, it is assumed that each agent is completely nonregular and has repeated operational characteristics in a finite time interval. At the ith iteration, the dynamics of the jth agent can be described as follows:

$$
\begin{cases}
{}_{0}^{C}D_t^{\alpha}\mathbf{x}_{i,j}(t) = \mathbf{A}\mathbf{x}_{i,j}(t) + \mathbf{B}\mathbf{u}_{i,j}(t),\\
\mathbf{y}_{i,j}(t) = \mathbf{C}\mathbf{x}_{i,j}(t),
\end{cases}
\tag{15}
$$

where $t \in [0,T]$, ${}_{0}^{C}D_t^{\alpha}\mathbf{x}_{i,j}(t)$ is the left-sided α-order derivative of $\mathbf{x}_{i,j}(t)$, $\alpha \in (0,1)$. $\mathbf{x}_{i,j}(t) \in \mathbb{R}^m$ is the state vectors, $\mathbf{u}_{i,j}(t) \in \mathbb{R}^{m1}$ and $\mathbf{y}_{i,j}(t) \in \mathbb{R}^{m2}$ are the input and output vectors, respectively, and $\mathbf{A}, \mathbf{B}, \mathbf{C}$ are constant matrices with $m \times m$, $m \times m1$, and $m2 \times m$.

The expected trajectory $\mathbf{y}_d(t)$ on the finite-time interval $[0,T]$ is generated by the virtual leader and it is described as

$$
\begin{cases}
{}_{0}^{C}D_t^{\alpha}\mathbf{x}_d(t) = \mathbf{A}\mathbf{x}_d(t) + \mathbf{B}\mathbf{u}_d(t),\\
\mathbf{y}_d(t) = \mathbf{C}\mathbf{x}_d(t),
\end{cases}
\tag{16}
$$

where $\mathbf{u}_d(t)$ is the desired control input, and it is continuous and unique control input.

If the virtual leader is the agent 0, the new graph can be expressed as $\overline{\mathbb{G}} = \{0 \cup \mathbb{V}, \overline{\mathbb{E}}, \overline{M}\}$, where $\overline{\mathbb{E}}$ and $\overline{M}$ are the new edge set and the new adjacency matrix of $\overline{\mathbb{G}}$. The purpose is to design appropriate FOILC algorithms that enable each agent in the network topology to track the leader's trajectory over a finite time interval.

$\xi_{i,j}(t)$ is defined as the distributed information of the jth agent, which is measured or received from other agents at the ith iteration. Consider

$$
\boldsymbol{\xi}_{i,j}(t) = \sum_{k\in\mathbf{N}_j} a_{j,k}\left(\mathbf{y}_{i,k}(t) - \mathbf{y}_{i,j}(t)\right) + s_j\left(\mathbf{y}_d(t) - \mathbf{y}_{i,j}(t)\right), \tag{17}
$$

where $a_{j,k}$ is the entry of adjacency matrix $\mathbf{M}$, $s_j = 1$ if the jth agent can obtain the desired trajectory, and $s_j = 0$ otherwise.

The tracking error of the jth agent is defined as $\mathbf{e}_{i,j}(t) = \mathbf{y}_d(t) - \mathbf{y}_{i,j}(t)$. Then, equation (17) can be reorganized as

$$
\boldsymbol{\xi}_{i,j}(t) = \sum_{k\in\mathbf{N}_j} a_{j,k}\left(\mathbf{e}_{i,j}(t) - \mathbf{e}_{i,k}(t)\right) + s_j\mathbf{e}_{i,j}(t). \tag{18}
$$

Define column stack vectors in the ith iteration

$$
\begin{cases}
\mathbf{x}_i(t) = \left[\mathbf{x}_{i,1}(t)^T, \mathbf{x}_{i,2}(t)^T, \ldots, \mathbf{x}_{i,N}(t)^T\right]^T,\\
\mathbf{e}_i(t) = \left[\mathbf{e}_{i,1}(t)^T, \mathbf{e}_{i,2}(t)^T, \ldots, \mathbf{e}_{i,N}(t)^T\right]^T,\\
\mathbf{u}_i(t) = \left[\mathbf{u}_{i,1}(t)^T, \mathbf{u}_{i,2}(t)^T, \ldots, \mathbf{u}_{i,N}(t)^T\right]^T,\\
\boldsymbol{\xi}_i(t) = \left[\boldsymbol{\xi}_{i,1}(t)^T, \boldsymbol{\xi}_{i,2}(t)^T, \ldots, \boldsymbol{\xi}_{i,N}(t)^T\right]^T.
\end{cases}
\tag{19}
$$

According to (19), (18) can be reorganized in a compact form

$$
\boldsymbol{\xi}_i(t) = \left((\mathbf{L} + \mathbf{S}) \otimes \mathbf{I}_m\right)\mathbf{e}_i(t), \tag{20}
$$

where L is the Laplacian matrix of graph $\mathbb{G}$, $\mathbf{I}_m$ is unit matrix, and $\mathbf{S} = \mathrm{diag}\{s_j, j \in \mathbb{S}_N\}$.

Similarly, equation (15) can be rearranged as

$$\begin{cases} {}_0^C D_t^\alpha \mathbf{x}_i(t) = (\mathbf{I}_N \otimes \mathbf{A})\mathbf{x}_i(t) + (\mathbf{I}_N \otimes \mathbf{B})\mathbf{u}_i(t). \\ \mathbf{y}_i(t) = (\mathbf{I}_N \otimes \mathbf{C})\mathbf{x}_i(t). \end{cases} \tag{21}$$

3.1. Open-Loop PD$^\alpha$-type FOILC. For FOMASs described by (15), considering the nonzero initial state, the open-loop PD$^\alpha$-type FOILC algorithm with initial state learning is proposed as follows:

$$\begin{cases} \mathbf{u}_{i+1,j}(t) = \mathbf{u}_{i,j}(t) + \Gamma_{P1}\boldsymbol{\xi}_{i,j}(t) + \Gamma_{D1}{}_0^C D_t^\alpha \boldsymbol{\xi}_{i,j}(t), \\ \mathbf{x}_{i+1,j}(0) = \mathbf{x}_{i,j}(0) + \mathbf{B}\Gamma_{D1}\boldsymbol{\xi}_{i,j}(0). \end{cases} \tag{22}$$

Similar to (20), the updating law (22) can be rewritten as

$$\begin{cases} \mathbf{u}_{i+1}(t) = \mathbf{u}_i(t) + ((\mathbf{L}+\mathbf{S}) \otimes \Gamma_{P1})\mathbf{e}_i(t) + ((\mathbf{L}+\mathbf{S}) \otimes \Gamma_{D1})_0^C D_t^\alpha \mathbf{e}_i(t), \\ \mathbf{x}_{i+1}(0) = \mathbf{x}_i(0) + ((\mathbf{L}+\mathbf{S}) \otimes \mathbf{B}\Gamma_{D1})\mathbf{e}_i(0). \end{cases} \tag{23}$$

In order to facilitate the convergence analysis of the proposed methods, the following assumptions hold.

Assumption 1. CB is of full column rank.

Remark 1. In order to guarantee the flawless tracking performance, a typical supposition, i.e., identical initialization condition, is needed to be made in the ILC design. Remember that accurate tracking can only be accomplished with perfect initial conditions.

Assumption 2 (see [17]). The graph $\overline{\mathbb{G}}$ contains a spanning tree with the leader being the root.

Remark 2. This supposition is a prerequisite for the FOMASs consensus tracking problem, which means all followers can receive the leader's information directly or indirectly. Otherwise, due to the absence of data to make their control inputs accurate, the isolated agents cannot keep track of the leader's trajectory.

Theorem 1. *Consider the FOMASs (15) and under the communication graph $\overline{\mathbb{G}}$, if Assumption 1 and 2 are satisfied. Distributed PD$^\alpha$-type updating rule (23) is applied to the FOMASs (15). If the matrices $\mathbf{A}, \mathbf{B}, \mathbf{C}$ and the learning gains Γ_{P1} and Γ_{D1} satisfy the following condition:*

$$\rho_1 = \left\| \mathbf{I} - (\mathbf{L}+\mathbf{S}) \otimes \mathbf{C}\mathbf{B}\Gamma_{D1} \right\| + \beta < 1, \tag{24}$$

where $\beta = \|\mathbf{I}_N \otimes \mathbf{C}\| \|(\mathbf{L}+\mathbf{S}) \otimes (\mathbf{B}\Gamma_{P1} + \mathbf{A}\mathbf{B}\Gamma_{D1})\| \|\Phi_{\alpha,\alpha}(\mathbf{I}_N \otimes \mathbf{A}, t)\|_1$, *then* $\lim_{i\longrightarrow\infty} \|\mathbf{e}_{i+1}(t)\|_p = 0$. *Namely, the output $\mathbf{y}_i(t)$ converges uniformly to the desired trajectory $\mathbf{y}_d(t)$ as $i \longrightarrow \infty$.*

Proof. The convergence discussed is as follows.

Based on Lemma 4, we can write the FOMASs (15) as follows:

$$\begin{aligned} \mathbf{x}_i(t) = {} & \boldsymbol{\Phi}_{\alpha,1}(\mathbf{I}_N \otimes \mathbf{A}, t)\mathbf{x}_i(0) \\ & + \int_0^t \boldsymbol{\Phi}_{\alpha,\alpha}(\mathbf{I}_N \otimes \mathbf{A}, t-\tau)(\mathbf{I}_N \otimes \mathbf{B})\mathbf{u}_i(\tau)\mathrm{d}\tau. \end{aligned} \tag{25}$$

According to equalities (21), (23), and (25), we can obtain

$$\begin{aligned} \mathbf{e}_{i+1}(t) &= \mathbf{1}_N \otimes \mathbf{y}_d(t) - \mathbf{y}_{i+1}(t) \\ &= (\mathbf{1}_N \otimes \mathbf{y}_d(t) - \mathbf{y}_i(t)) - (\mathbf{y}_{i+1}(t) - \mathbf{y}_i(t)) \\ &= \mathbf{e}_i(t) - (\mathbf{I}_N \otimes \mathbf{C})(\mathbf{x}_{i+1}(t) - \mathbf{x}_i(t)) \\ &= \mathbf{e}_i(t) - (\mathbf{I}_N \otimes \mathbf{C})\Phi_{\alpha,1}(\mathbf{I}_N \otimes \mathbf{A}, t)(\mathbf{x}_{i+1}(0) - \mathbf{x}_i(0)) \\ &\quad - (\mathbf{I}_N \otimes \mathbf{C})\int_0^t \Phi_{\alpha,\alpha}(\mathbf{I}_N \otimes \mathbf{A}, t-\tau)(\mathbf{I}_N \otimes \mathbf{B})(\mathbf{u}_{i+1}(\tau) - \mathbf{u}_i(\tau))\mathrm{d}\tau \\ &= \mathbf{e}_i(t) - (\mathbf{I}_N \otimes \mathbf{C})\Phi_{\alpha,1}(\mathbf{I}_N \otimes \mathbf{A}, t)((\mathbf{L}+\mathbf{S}) \otimes \mathbf{B}\Gamma_{D1})\mathbf{e}_i(0) \\ &\quad - (\mathbf{I}_N \otimes \mathbf{C})\int_0^t \Phi_{\alpha,\alpha}(\mathbf{I}_N \otimes \mathbf{A}, t-\tau)(\mathbf{I}_N \otimes \mathbf{B})((\mathbf{L}+\mathbf{S}) \otimes \Gamma_{P1})\mathbf{e}_i(\tau)\mathrm{d}\tau \\ &\quad - (\mathbf{I}_N \otimes \mathbf{C})\int_0^t \Phi_{\alpha,\alpha}(\mathbf{I}_N \otimes \mathbf{A}, t-\tau)(\mathbf{I}_N \otimes \mathbf{B})((\mathbf{L}+\mathbf{S}) \otimes \Gamma_{D1})_0^C D_T^\alpha \mathbf{e}_i(t)\mathrm{d}\tau \\ &= \mathbf{e}_i(t) - (\mathbf{I}_N \otimes \mathbf{C})\Phi_{\alpha,1}(\mathbf{I}_N \otimes \mathbf{A}, t)((\mathbf{L}+\mathbf{S}) \otimes \mathbf{B}\Gamma_{D1})\mathbf{e}_i(0) \\ &\quad - (\mathbf{I}_N \otimes \mathbf{C})\int_0^t \Phi_{\alpha,\alpha}(\mathbf{I}_N \otimes \mathbf{A}, t-\tau)((\mathbf{L}+\mathbf{S}) \otimes \mathbf{B}\Gamma_{P1})\mathbf{e}_i(\tau)\mathrm{d}\tau \\ &\quad - (\mathbf{I}_N \otimes \mathbf{C})\int_0^t \Phi_{\alpha,\alpha}(\mathbf{I}_N \otimes \mathbf{A}, t-\tau)((\mathbf{L}+\mathbf{S}) \otimes \mathbf{B}\Gamma_{D1})_0^C D_T^\alpha \mathbf{e}_i(\tau)\mathrm{d}\tau \end{aligned} \tag{26}$$

where $\mathbf{1}_{(\cdot)}$ is a vector in which all entries are 1.

From Lemma 2 and 3, we can see that

$$\begin{aligned}
&\int_0^t \Phi_{\alpha,\alpha}(\mathbf{I}_N \otimes \mathbf{A}, t-\tau)\left((\mathbf{L}+\mathbf{S})\otimes \mathbf{B}\Gamma_{D1}\right){}_0^C D_t^{\alpha}\mathbf{e}_i(t)\mathrm{d}\tau \\
&= \int_0^t {}_\tau^C D_t^{1-\alpha}\left(\Phi_{\alpha,1}(\mathbf{I}_N \otimes \mathbf{A}, t-\tau)\right)\left((\mathbf{L}+\mathbf{S})\otimes \mathbf{B}\Gamma_{D1}\right){}_0^C D_t^{\alpha}\mathbf{e}_i(t)\mathrm{d}\tau \\
&= \int_0^t \Phi_{\alpha,1}(\mathbf{I}_N \otimes \mathbf{A}, t-\tau)\left((\mathbf{L}+\mathbf{S})\otimes \mathbf{B}\Gamma_{D1}\right){}_0^C D_t^{1-\alpha}\left({}_0^C D_t^{\alpha}\mathbf{e}_i(t)\right)\mathrm{d}\tau \\
&= \int_0^t \Phi_{\alpha,1}(\mathbf{I}_N \otimes \mathbf{A}, t-\tau)\left((\mathbf{L}+\mathbf{S})\otimes \mathbf{B}\Gamma_{D1}\right)\mathbf{e}_i'(\tau)\mathrm{d}\tau \\
&= \int_0^t \Phi_{\alpha,1}(\mathbf{I}_N \otimes \mathbf{A}, t-\tau)\left((\mathbf{L}+\mathbf{S})\otimes \mathbf{B}\Gamma_{D1}\right)\mathrm{d}\mathbf{e}_i(\tau) \\
&= \Phi_{\alpha,1}(\mathbf{I}_N \otimes \mathbf{A}, t-\tau)\left((\mathbf{L}+\mathbf{S})\otimes \mathbf{B}\Gamma_{D1}\right)\mathbf{e}_i(\tau)|_0^t \\
&\quad - \int_0^t \frac{\mathrm{d}}{\mathrm{d}\tau}\left(\Phi_{\alpha,1}(\mathbf{I}_N \otimes \mathbf{A}, t-\tau)\left((\mathbf{L}+\mathbf{S})\otimes \mathbf{B}\Gamma_{D1}\right)\right)\mathbf{e}_i(\tau)\mathrm{d}\tau \\
&= \Phi_{\alpha,1}(\mathbf{I}_N \otimes \mathbf{A}, 0)\left((\mathbf{L}+\mathbf{S})\otimes \mathbf{B}\Gamma_{D1}\right)\mathbf{e}_i(t) \\
&\quad - \Phi_{\alpha,1}(\mathbf{I}_N \otimes \mathbf{A}, t)\left((\mathbf{L}+\mathbf{S})\otimes \mathbf{B}\Gamma_{D1}\right)\mathbf{e}_i(0) \\
&\quad + \int_0^t \Phi_{\alpha,1}(\mathbf{I}_N \otimes \mathbf{A}, t-\tau)\left(\mathbf{I}_N \otimes \mathbf{A}\right)\left(\mathbf{I}_N \otimes \mathbf{B}\right)\left((\mathbf{L}+\mathbf{S})\otimes \Gamma_{D1}\right)\mathbf{e}_i(\tau)\mathrm{d}\tau \\
&= \left((\mathbf{L}+\mathbf{S})\otimes \mathbf{B}\Gamma_{D1}\right)\mathbf{e}_i(t) - \Phi_{\alpha,1}(\mathbf{I}_N \otimes \mathbf{A}, t)\left((\mathbf{L}+\mathbf{S})\otimes \mathbf{B}\Gamma_{D1}\right)\mathbf{e}_i(0) \\
&\quad + \int_0^t \Phi_{\alpha,1}(\mathbf{I}_N \otimes \mathbf{A}, t-\tau)\left((\mathbf{L}+\mathbf{S})\otimes \mathbf{A}\mathbf{B}\Gamma_{D1}\right)\mathbf{e}_i(\tau)\mathrm{d}\tau.
\end{aligned} \tag{27}$$

Taking (27) into (26), we further get

$$\begin{aligned}
\mathbf{e}_{i+1}(t) &= \left(\mathbf{I} - \left(\mathbf{I}_N \otimes \mathbf{C}\right)\left((\mathbf{L}+\mathbf{S})\otimes \mathbf{B}\Gamma_{D1}\right)\mathbf{e}_i(t)\right. \\
&\quad - \left(\mathbf{I}_N \otimes \mathbf{C}\right)\int_0^t \Phi_{\alpha,\alpha}(\mathbf{I}_N \otimes \mathbf{A}, t-\tau)\left((\mathbf{L}+\mathbf{S})\otimes \mathbf{B}\Gamma_{P1}\right)\mathbf{e}_i(\tau)\mathrm{d}\tau \\
&\quad - \left(\mathbf{I}_N \otimes \mathbf{C}\right)\int_0^t \Phi_{\alpha,1}(\mathbf{I}_N \otimes \mathbf{A}, t-\tau)\left((\mathbf{L}+\mathbf{S})\otimes \mathbf{A}\mathbf{B}\Gamma_{D1}\right)\mathbf{e}_i(\tau)\mathrm{d}\tau \\
&= \left(\mathbf{I} - (\mathbf{L}+\mathbf{S})\otimes \mathbf{C}\mathbf{B}\Gamma_{D1}\right)\mathbf{e}_i(t) - \left(\mathbf{I}_N \otimes \mathbf{C}\right)\int_0^t \Phi_{\alpha,\alpha}(\mathbf{I}_N \otimes \mathbf{A}, t-\tau)\left((\mathbf{L}+\mathbf{S})\otimes \left(\mathbf{B}\Gamma_{P1} + \mathbf{A}\mathbf{B}\Gamma_{D1}\right)\right)\mathbf{e}_i(\tau)\mathrm{d}\tau.
\end{aligned} \tag{28}$$

According to Lemma 1, taking Lebesgue-p norm on both sides of (28), we achieve

$$\left\|\mathbf{e}_{i+1}(t)\right\|_p \le \left(\left\|\mathbf{I} - (\mathbf{L}+\mathbf{S})\otimes \mathbf{C}\mathbf{B}\Gamma_{D1}\right\| + \beta\right)\left\|\mathbf{e}_i(t)\right\|_p = \rho_1\left\|\mathbf{e}_i(t)\right\|_p, \tag{29}$$

where

$$\beta = \left\|\mathbf{I}_N \otimes \mathbf{C}\right\|\left\|(\mathbf{L}+\mathbf{S})\otimes \left(\mathbf{B}\Gamma_{P1} + \mathbf{A}\mathbf{B}\Gamma_{D1}\right)\right\|\left\|\Phi_{\alpha,\alpha}(\mathbf{I}_N \otimes \mathbf{A}, t)\right\|_1. \tag{30}$$

Recalling the condition of $\rho < 1$, it deduces that

$$\left\|\mathbf{e}_{i+1}(t)\right\|_p \le \rho_1\left\|\mathbf{e}_i(t)\right\|_p \le \rho_1^i\left\|\mathbf{e}_1(t)\right\|_p. \tag{31}$$

So, as the iterations number increases, i.e., $i \longrightarrow \infty$, we obtain

$$\lim_{i\longrightarrow\infty}\left\|\mathbf{e}_{i+1}(t)\right\|_p = 0. \tag{32}$$

It shows that the tracking errors of all the agents tend to reach zero in finite time when $i \longrightarrow \infty$. The proof is completed. When $\Gamma_{P1} = 0$, the open-loop PD$^{\alpha}$-type fractional-order algorithm degenerates into the D^{α}-type fractional-order algorithm, which has the following form:

$$\mathbf{u}_{i+1}(t) = \mathbf{u}_i(t) + \left((\mathbf{L}+\mathbf{S})\otimes\Gamma_{D1}\right)\mathbf{e}_i^{(\alpha)}(t). \tag{33}$$

Thus, the following corollary can be obtained. □

Corollary 1. *Consider the FOMASs (15) and under the communication graph $\overline{\mathbb{G}}$, if Assumptions 1 and 2 are satisfied. Distributed Dα-type updating rule (33) is applied to the FOMASs (15). Assuming that*

$$\left\|\mathbf{I} - (\mathbf{L}+\mathbf{S})\otimes\mathbf{CB}\Gamma_{D1}\right\| + \beta_0 < 1 \tag{34}$$

holds for all [0, T], where $\beta_0 = \|\mathbf{I}_N\otimes\mathbf{C}\|\|(\mathbf{L}+\mathbf{S})\otimes\mathbf{AB}\Gamma_{D1}\|\|\Phi_{\alpha,\alpha}(\mathbf{I}_N\otimes\mathbf{A},t)\|_1$, then $\lim_{i\longrightarrow\infty}\|\mathbf{e}_{i+1}(t)\|_p = 0$. Namely, the output $\mathbf{y}_i(t)$ converges uniformly to the desired trajectory $\mathbf{y}_d(t)$ as $i\longrightarrow\infty$.

Proof. The process of proof is similar to Theorem 1. □

3.2. Closed-Loop PD$^\alpha$ -Type FOILC. The closed-loop PD$^\alpha$ -type FOILC updating law for the FOMASs (15) is designed as follows:

$$\begin{cases} \mathbf{u}_{i+1,j}(t) = \mathbf{u}_{i,j}(t) + \Gamma_{P2}\boldsymbol{\xi}_{i+1,j}(t) + \Gamma_{D20}{}^{C}D_t^{\alpha}\boldsymbol{\xi}_{i+1,j}(t), \\ \mathbf{x}_{i+1,j}(0) = \mathbf{x}_{i,j}(0) + \mathbf{B}\Gamma_{D2}\boldsymbol{\xi}_{i+1,j}(0). \end{cases} \tag{35}$$

Similar to (23), the updating law (35) can be rewritten by the Kronecker product as

$$\begin{cases} \mathbf{u}_{i+1}(t) = \mathbf{u}_i(t) + \left((\mathbf{L}+\mathbf{S})\otimes\Gamma_{P2}\right)\mathbf{e}_{i+1}(t) + \left((\mathbf{L}+\mathbf{S})\otimes\Gamma_{D2}\right){}_0^{C}D_t^{\alpha}\mathbf{e}_{i+1}(t), \\ \mathbf{x}_{i+1}(0) = \mathbf{x}_i(0) + \left((\mathbf{L}+\mathbf{S})\otimes\mathbf{B}\Gamma_{D2}\right)\mathbf{e}_{i+1}(0), \end{cases} \tag{36}$$

where $\mathbf{L}$ and $\mathbf{S}$ are the same as defined in (20).

Theorem 2. *Consider the FOMASs (15) under a directed graph $\overline{\mathbb{G}}$, if Assumptions 1 and 2 hold. The closed-loop PD$^\alpha$-type FOILC described in (36) is applied for the system (15). If learning gains Γ_{P2} and Γ_{D2} satisfy*

$$0 < \rho_2 = \left(\frac{1}{\left\|\left(\mathbf{I}+(\mathbf{L}+\mathbf{S})\otimes\mathbf{CB}\Gamma_{D2}\right)^{-1}\right\|} - \gamma\right)^{-1} < 1, \tag{37}$$

where

$$\gamma = \left\|\mathbf{I}_N\otimes\mathbf{C}\right\|\left\|(\mathbf{L}+\mathbf{S})\otimes\left(\mathbf{B}\Gamma_{P2}+\mathbf{AB}\Gamma_{D2}\right)\right\|\left\|\boldsymbol{\Phi}_{\alpha,\alpha}\left(\mathbf{I}_N\otimes\mathbf{A},t\right)\right\|_1, \tag{38}$$

then $\lim_{i\longrightarrow\infty}\|\mathbf{e}_{i+1}(t)\|_p = 0$. Hence, the system outputs $\mathbf{y}_i(t)$ can fully track the desired trajectory $\mathbf{y}_d(t)$ in a finite time when $i\longrightarrow\infty$ for all $t\in[0,T]$; that is, $\lim_{i\longrightarrow\infty}\mathbf{y}_i(t) = \mathbf{y}_d(t)$, $(t\in[0,T])$.

Proof. From (15) and (36), we can get

$$\begin{aligned} \mathbf{e}_{i+1}(t) &= \mathbf{e}_i(t) - \left(\mathbf{I}_N\otimes\mathbf{C}\right)\left(\mathbf{x}_{i+1}(t)-\mathbf{x}_i(t)\right) = \mathbf{e}_i(t) - \left(\mathbf{I}_N\otimes\mathbf{C}\right)\Phi_{\alpha,1}\left(\mathbf{I}_N\otimes\mathbf{A},t\right)\left(\mathbf{x}_{i+1}(0)-\mathbf{x}_i(0)\right) \\ &\quad - \left(\mathbf{I}_N\otimes\mathbf{C}\right)\int_0^t\Phi_{\alpha,\alpha}\left(\mathbf{I}_N\otimes\mathbf{A},t-\tau\right)\left(\mathbf{I}_N\otimes\mathbf{B}\right)\left(\mathbf{u}_{i+1}(\tau)-\mathbf{u}_i(\tau)\right)\mathrm{d}\tau \\ &= \mathbf{e}_i(t) - \left(\mathbf{I}_N\otimes\mathbf{C}\right)\Phi_{\alpha,1}\left(\mathbf{I}_N\otimes\mathbf{A},t\right)\left((\mathbf{L}+\mathbf{S})\otimes\mathbf{B}\Gamma_{D2}\right)\mathbf{e}_{i+1}(0) \\ &\quad - \left(\mathbf{I}_N\otimes\mathbf{C}\right)\int_0^t\Phi_{\alpha,\alpha}\left(\mathbf{I}_N\otimes\mathbf{A},t-\tau\right)\left((\mathbf{L}+\mathbf{S})\otimes\mathbf{B}\Gamma_{P2}\right)\mathbf{e}_{i+1}(\tau)\mathrm{d}\tau \\ &\quad - \left(\mathbf{I}_N\otimes\mathbf{C}\right)\int_0^t\Phi_{\alpha,\alpha}\left(\mathbf{I}_N\otimes\mathbf{A},t-\tau\right)\left((\mathbf{L}+\mathbf{S})\otimes\mathbf{B}\Gamma_{D2}\right){}_0^{C}D_t^{\alpha}\mathbf{e}_{i+1}(t)\mathrm{d}\tau, \end{aligned} \tag{39}$$

where $\mathbf{1}_{(\cdot)}$ is a vector in which all entries are 1.

Similar to the derivation of (27), one can conclude that

$$\begin{aligned} \int_0^t\Phi_{\alpha,\alpha}\left(\mathbf{I}_N\otimes\mathbf{A},t-\tau\right)\left((\mathbf{L}+\mathbf{S})\otimes\mathbf{B}\Gamma_{D2}\right){}_0^{C}D_t^{\alpha}\mathbf{e}_{i+1}(t)\mathrm{d}\tau &= \left((\mathbf{L}+\mathbf{S})\otimes\mathbf{B}\Gamma_{D2}\right)\mathbf{e}_{i+1}(t) - \Phi_{\alpha,1}\left(\mathbf{I}_N\otimes\mathbf{A},t\right)\left((\mathbf{L}+\mathbf{S})\otimes\mathbf{B}\Gamma_{D2}\right)\mathbf{e}_{i+1}(0) \\ &\quad + \int_0^t\Phi_{\alpha,1}\left(\mathbf{I}_N\otimes\mathbf{A},t-\tau\right)\left((\mathbf{L}+\mathbf{S})\otimes\mathbf{AB}\Gamma_{D2}\right)\mathbf{e}_{i+1}(\tau)\mathrm{d}\tau. \end{aligned} \tag{40}$$

Substituting (40) into (39), it yields

$$\begin{aligned}\mathbf{e}_{i+1}(t) &= \mathbf{e}_i(t) - (\mathbf{I}_N \otimes \mathbf{C})((\mathbf{L}+\mathbf{S}) \otimes \mathbf{B}\Gamma_{D2})\mathbf{e}_{i+1}(t) \\ &\quad - (\mathbf{I}_N \otimes \mathbf{C}) \int_0^t \Phi_{\alpha,\alpha}(\mathbf{I}_N \otimes \mathbf{A}, t-\tau)((\mathbf{L}+\mathbf{S}) \otimes \mathbf{B}\Gamma_{P2})\mathbf{e}_{i+1}(\tau)\mathrm{d}\tau \\ &\quad - (\mathbf{I}_N \otimes \mathbf{C}) \int_0^t \Phi_{\alpha,1}(\mathbf{I}_N \otimes \mathbf{A}, t-\tau)((\mathbf{L}+\mathbf{S}) \otimes \mathbf{AB}\Gamma_{D2})\mathbf{e}_{i+1}(\tau)\mathrm{d}\tau \\ &= \mathbf{e}_i(t) - ((\mathbf{L}+\mathbf{S}) \otimes \mathbf{CB}\Gamma_{D2})\mathbf{e}_{i+1}(\tau) - (\mathbf{I}_N \otimes \mathbf{C}) \\ &\quad \cdot \int_0^t \Phi_{\alpha,\alpha}(\mathbf{I}_N \otimes \mathbf{A}, t-\tau)((\mathbf{L}+\mathbf{S}) \otimes (\mathbf{B}\Gamma_{P2} + \mathbf{AB}\Gamma_{D2}))\mathbf{e}_{i+1}(\tau)\mathrm{d}\tau.\end{aligned} \tag{41}$$

Therefore,

$$\begin{aligned}&(\mathbf{I} + (\mathbf{L}+\mathbf{S}) \otimes \mathbf{CB}\Gamma_{D2})\mathbf{e}_{i+1}(t) \\ &= \mathbf{e}_i(t) - (\mathbf{I}_N \otimes \mathbf{C}) \int_0^t \Phi_{\alpha,\alpha}(\mathbf{I}_N \otimes \mathbf{A}, t-\tau)((\mathbf{L}+\mathbf{S}) \\ &\quad \otimes (\mathbf{B}\Gamma_{P2} + \mathbf{AB}\Gamma_{D2}))\mathbf{e}_{i+1}(\tau)\mathrm{d}\tau.\end{aligned} \tag{42}$$

According to Assumption 1, one can find a feedback gain matrix of differentiation Γ_{D2} such that $\mathbf{I} + (\mathbf{L}+\mathbf{S}) \otimes \mathbf{CB}\Gamma_{D2}$ is a nonsingular matrix. Therefore, premultiplying by $(\mathbf{I} + (\mathbf{L}+\mathbf{S}) \otimes \mathbf{CB}\Gamma_{D2})^{-1}$ on both sides of (42), taking Lebesgue-p norm, and adopting the generalized Young inequality of convolution integral, it can be concluded that

$$\|\mathbf{e}_{i+1}(t)\|_p \le \left\|(\mathbf{I} + (\mathbf{L}+\mathbf{S}) \otimes \mathbf{CB}\Gamma_{D2})^{-1}\right\| \left(\|\mathbf{e}_i(t)\|_p + \lambda\|\mathbf{e}_{i+1}(t)\|_p\right), \tag{43}$$

where

$$\gamma = \|\mathbf{I}_N \otimes \mathbf{C}\| \|(\mathbf{L}+\mathbf{S}) \otimes (\mathbf{B}\Gamma_{P2} + \mathbf{AB}\Gamma_{D2})\| \|\Phi_{\alpha,\alpha}(\mathbf{I}_N \otimes \mathbf{A}, t)\|_1. \tag{44}$$

Further

$$\begin{aligned}\|\mathbf{e}_{i+1}(t)\|_p &\le \left(\frac{1}{\left\|(\mathbf{I} + (\mathbf{L}+\mathbf{S}) \otimes \mathbf{CB}\Gamma_{D2})^{-1}\right\|} - \gamma\right)^{-1} \|\mathbf{e}_i(t)\|_p \\ &= \rho_2 \|\mathbf{e}_i(t)\|_p.\end{aligned} \tag{45}$$

Recalling the condition of $\rho_2 < 1$, according to inequality (43), it is deduced that

$$\|\mathbf{e}_{i+1}(t)\|_p \le \rho_2 \|\mathbf{e}_i(t)\|_p \le \rho_2^i \|\mathbf{e}_1(t)\|_p. \tag{46}$$

From (45), when the number of iterations is large enough, i.e., $i \longrightarrow \infty$, we obtain

$$\lim_{i \longrightarrow \infty} \|\mathbf{e}_{i+1}(t)\|_p \longrightarrow 0. \tag{47}$$

So, it can be proved that the errors of all the fractional-order agents tend to zero as $i \longrightarrow \infty$. For the FOMASs (15), if $\Gamma_{P2} = 0$ in (37), then the PD$^\alpha$ -type FOILC will become D^α-type FOILC.

$$\mathbf{u}_{i+1}(t) = \mathbf{u}_i(t) + ((\mathbf{L}+\mathbf{S}) \otimes \Gamma_{D2})\mathbf{e}_{i+1}^{(\alpha)}(t). \tag{48}$$

Thus, according to Theorem 2, we can obtain a corollary as follows. □

Corollary 2. *For the FOMASs (15) under a directed graph $\overline{\mathbb{G}}$, suppose Assumptions 1 and 2 hold. If the learning gain Γ_{D2} in (48) is chosen such that*

$$\left(\frac{1}{\left\|(\mathbf{I} + (\mathbf{L}+\mathbf{S}) \otimes \mathbf{CB}\Gamma_{D2})^{-1}\right\|} - \gamma_0\right)^{-1} < 1, \tag{49}$$

where

$$\gamma_0 = \|\mathbf{I}_N \otimes \mathbf{C}\| \|(\mathbf{L}+\mathbf{S}) \otimes \mathbf{AB}\Gamma_{D2}\| \|\Phi_{\alpha,\alpha}(\mathbf{I}_N \otimes \mathbf{A}, t)\|_1. \tag{50}$$

Then the tracking error satisfies $\lim_{i \longrightarrow \infty} \|\mathbf{e}_{i+1}(t)\|_p = 0$. Namely, the outputs $\mathbf{y}_i(t)$ of the FOMASs (15) converge to the desired trajectory $\mathbf{y}_d(t)$ uniformly in a finite time when $i \longrightarrow \infty$, i.e., $\lim_{i \longrightarrow \infty} \mathbf{y}_i(t) = \mathbf{y}_d(t)$, $(t \in [0, T])$.

Proof. The proof process of the corollary is similar to Theorem 2. □

3.3. Open-Closed-Loop PD$^\alpha$-Type FOILC. Considering the FOMASs (15), an open-closed-loop PD$^\alpha$-type FOILC is designed as

$$\begin{cases}\mathbf{u}_{i+1,j}(t) = \mathbf{u}_{i,j}(t) + \Gamma_{P1}\boldsymbol{\xi}_{i,j}(t) + \Gamma_{D1}{}_0^C D_t^\alpha \boldsymbol{\xi}_{i,j}(t) + \Gamma_{P2}\boldsymbol{\xi}_{i+1,j}(t) + \Gamma_{D2}{}_0^C D_t^\alpha \boldsymbol{\xi}_{i+1,j}(t), \\ \mathbf{x}_{i+1,j}(0) = \mathbf{x}_{i,j}(0) + \mathbf{B}\left(\Gamma_{D1}\boldsymbol{\xi}_{i,j}(0) + \Gamma_{D2}\boldsymbol{\xi}_{i+1,j}(0)\right).\end{cases} \tag{51}$$

Similar to (25), the updating law (51) can be rewritten by the Kronecker product as

$$\begin{cases} \mathbf{u}_{i+1}(t) = \mathbf{u}_i(t) + ((\mathbf{L}+\mathbf{S})\otimes\Gamma_{P1})\mathbf{e}_i(t) + ((\mathbf{L}+\mathbf{S})\otimes\Gamma_{D1})\,{}_0^C D_t^{\alpha}\mathbf{e}_i(t) + ((\mathbf{L}+\mathbf{S})\otimes\Gamma_{P2})\mathbf{e}_{i+1}(t) + ((\mathbf{L}+\mathbf{S})\otimes\Gamma_{D2})\,{}_0^C D_t^{\alpha}\mathbf{e}_{i+1}(t), \\ \mathbf{x}_{i+1}(0) = \mathbf{x}_i(0) + (\mathbf{L}+\mathbf{S})\otimes\mathbf{B}\left(\Gamma_{D1}\mathbf{e}_i(0) + \Gamma_{D2}\mathbf{e}_{i+1}(0)\right), \end{cases} \tag{52}$$

where $\mathbf{L}$ and $\mathbf{S}$ are the same as defined in (20) and (36).

Theorem 3. *Consider the FOMASs (15) under a directed graph $\overline{\mathbb{G}}$, if Assumptions 1 and 2 hold. Let the distributed closed-loop PD$^{\alpha}$-type FOILC described in (52) be applied for the system with learning gains $\Gamma_{P1}\Gamma_{P2}$,Γ_{D1}, and Γ_{D2} satisfying*

$$\rho_2\rho_1 < 1, \tag{53}$$

where

$$\begin{aligned} \rho_1 &= \left\|\mathbf{I} - (\mathbf{L}+\mathbf{S})\otimes\mathbf{CB}\Gamma_{D1}\right\| + \beta, \\ \rho_2 &= \left(\frac{1}{\left\|\left(\mathbf{I} + (\mathbf{L}+\mathbf{S})\otimes\mathbf{CB}\Gamma_{D2}\right)^{-1}\right\|} - \gamma\right)^{-1} > 0, \\ \beta &= \left\|\mathbf{I}_N\otimes\mathbf{C}\right\|\left\|(\mathbf{L}+\mathbf{S})\otimes\left(\mathbf{B}\Gamma_{P1} + \mathbf{AB}\Gamma_{D1}\right)\right\|\left\|\Phi_{\alpha,\alpha}\left(\mathbf{I}_N\otimes\mathbf{A}, t\right)\right\|_1 \\ \gamma &= \left\|\mathbf{I}_N\otimes\mathbf{C}\right\|\left\|(\mathbf{L}+\mathbf{S})\otimes\left(\mathbf{B}\Gamma_{P2} + \mathbf{AB}\Gamma_{D2}\right)\right\|\left\|\Phi_{\alpha,\alpha}\left(\mathbf{I}_N\otimes\mathbf{A}, t\right)\right\|_1. \end{aligned} \tag{54}$$

Then $\lim_{i\longrightarrow\infty}\|\mathbf{e}_{i+1}(t)\|_p = 0$. Thus, the system outputs $\mathbf{y}_i(t)$ of the fractional-order agents converge to $\mathbf{y}_d(t)$ when $i \longrightarrow \infty$ for all $t \in [0,T]$; that is, $\lim_{i\longrightarrow\infty}\mathbf{y}_i(t) = \mathbf{y}_d(t)$, $(t \in [0,T])$.

Remark 3. According to the conditions of Theorems 1 and 2, in the sense of Lebesgue-p norm, the convergence conditions of the proposed algorithms are determined by the learning gain and the properties of the system.

4. Simulation

In this section, five fractional-order agents are considered, including a virtual leader and four followers. The directed fixed communication topology among agents is shown in Figure 1, where the fractional-order agents are labeled with 0, 1, 2, 3, and 4, respectively. The virtual leader has directed edges to agents 1 and 3.

From Figure 1, the Laplacian matrix $\mathbf{L}$ and the information transfer matrix $\mathbf{S}$ of the leader to the followers can be obtained as follows:

$$\mathbf{L} = \begin{bmatrix} 1 & -1 & 0 & 0 \\ -1 & 2 & 0 & -1 \\ 0 & 0 & 1 & -1 \\ 0 & -1 & -1 & 2 \end{bmatrix}, \qquad \mathbf{S} = \operatorname{diag}(1,0,1,0). \tag{55}$$

The dynamic model of the jth agent is described as

$$\begin{cases} D^{\alpha}\mathbf{x}_j(t) = \begin{bmatrix} 0.4 & 2 \\ 5 & -6 \end{bmatrix}\mathbf{x}_j(t) + \begin{bmatrix} 1 & 0 \\ 0 & 1 \end{bmatrix}\mathbf{u}_j(t), \\ \mathbf{y}_j(t) = \begin{bmatrix} 0.85 & 0 \\ 0 & 1 \end{bmatrix}\mathbf{x}_j(t), \end{cases} \tag{56}$$

Here, $t \in [0,1]$, $\alpha = 0.75$.

Let the virtual leader be the given expected reference trajectory

$$\begin{cases} y_{d1} = t^2 + \sin(2\pi t), & (t \in [0,1]), \\ y_{d2} = \sin(2\pi t), & (t \in [0,1]). \end{cases} \tag{57}$$

In the following simulations, the initial states of the followers at first iteration are set as $x_{0,1} = \begin{bmatrix} 0.1 & 0.3 \end{bmatrix}^T$, $x_{0,2} = \begin{bmatrix} -0.5 & -0.7 \end{bmatrix}^T$, $x_{0,3} = \begin{bmatrix} 0.2 & 0.4 \end{bmatrix}^T$, and $x_{0,4} = \begin{bmatrix} -0.6 & 0.8 \end{bmatrix}^T$. The control objective of the initial state is $x_d = \begin{bmatrix} 0 & 0 \end{bmatrix}^T$ and the initial control is set as $\mathbf{u}_{0,j}(t) = 0$, $j = 1,2,3,4$ for all agents.

Case 1. Open-loop PD$^{\alpha}$-type: the open-loop PD$^{\alpha}$-type is applied to the multiagent system (1). Based on Theorem 1, the gains are selected as $\Gamma_{P1} = \begin{bmatrix} 0.4 & 0 \\ 0 & 0.6 \end{bmatrix}$,$\Gamma_{D1} = \begin{bmatrix} 0.2 & 0 \\ 0 & 0.3 \end{bmatrix}$. Thus, we can calculate $\rho_1 = \|\mathbf{I} - ((\mathbf{L}+\mathbf{D})\otimes\Gamma_{D1}\mathbf{CB})\| + \beta_1 = 0.9421 < 1$, which satisfies the convergence condition (26).

The simulation results are shown in Figures 2–4. The initial states of the followers at the first iteration are $x_{0,1} = \begin{bmatrix} 0.1 & 0.3 \end{bmatrix}^T$, $x_{0,2} = \begin{bmatrix} -0.5 & -0.7 \end{bmatrix}^T$, $x_{0,3} = \begin{bmatrix} 0.2 & 0.4 \end{bmatrix}^T$, and $x_{0,4} = \begin{bmatrix} -0.6 & 0.8 \end{bmatrix}^T$. And the desired initial states of the four followers are zero; that is $x_{0,j} = \begin{bmatrix} 0 & 0 \end{bmatrix}^T$ for $j = 1, 2, 3, 4$. Figure 2 shows the initial state learning process. It can be seen that the initial states $x1$ and $x2$ of the multiagent at time zero have a large error from the desired state at the beginning of the iteration, because the initial control is set as $\mathbf{u}_{0,j}(t) = 0$, $j = 1,2,3,4$ for all agents. But as the number of iterations increases, the errors of the initial states gradually decrease. When the number of iterations reaches the 40th iteration, the initial state of $x2$ also converges to the desired initial state. And when the number of iterations reaches the 60th iteration, the initial state of $x1$ converges to the desired initial state. Figure 3 shows the output tracking results of $y1$ and $y2$. It can be seen that each subsystem does not track the desired trajectory at the 5th iteration. With the increase of the number of iterations, when it reaches the 100th iteration, both the outputs $y1$ and $y2$ of all the agents fully track the

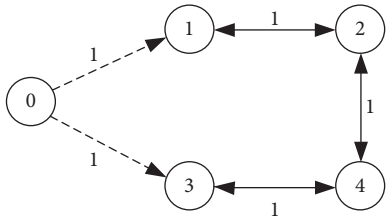

Figure 1: Communication graph among agents in the network.

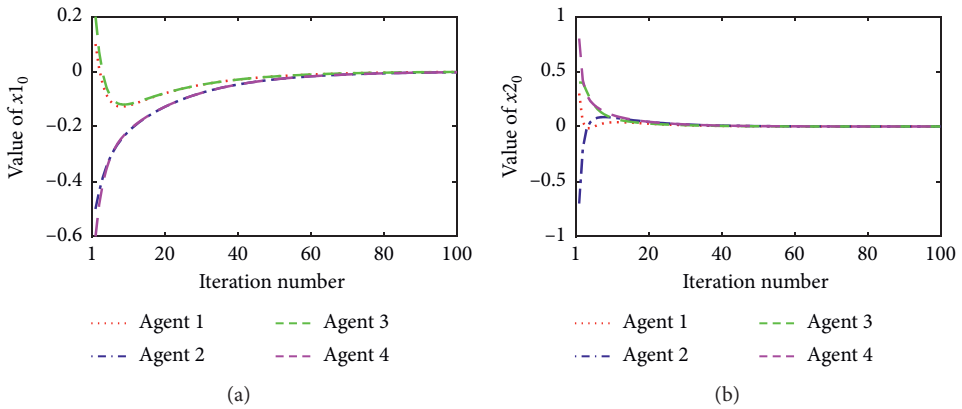

Figure 2: Initial state profile vs. iteration number by open-loop PD$^{\alpha}$-type. (a) Initial state learning of $x1$. (b) Initial state learning of $x2$.

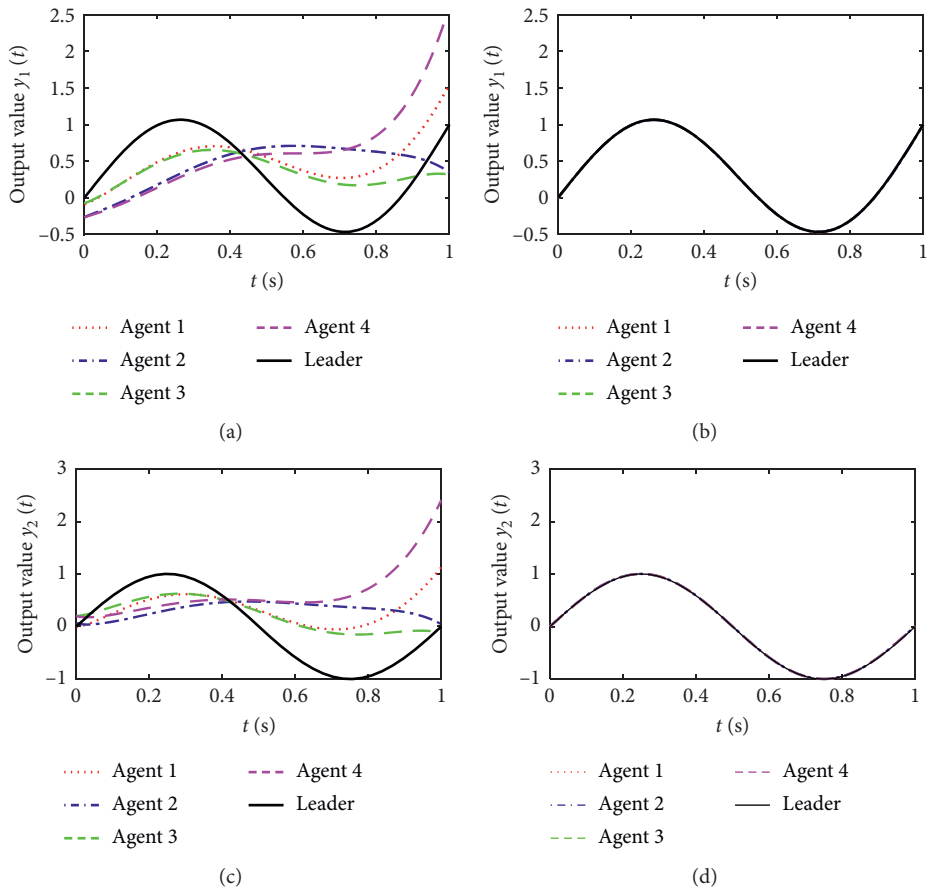

Figure 3: The tracking results of all agents at different iterations by open-loop PD$^{\alpha}$-type. (a) Output $y1$ at the 5th iteration. (b) Output $y1$ at the 100th iteration. (c) Output $y2$ at the 5th iteration. (d) Output $y2$ at the 100th iteration.

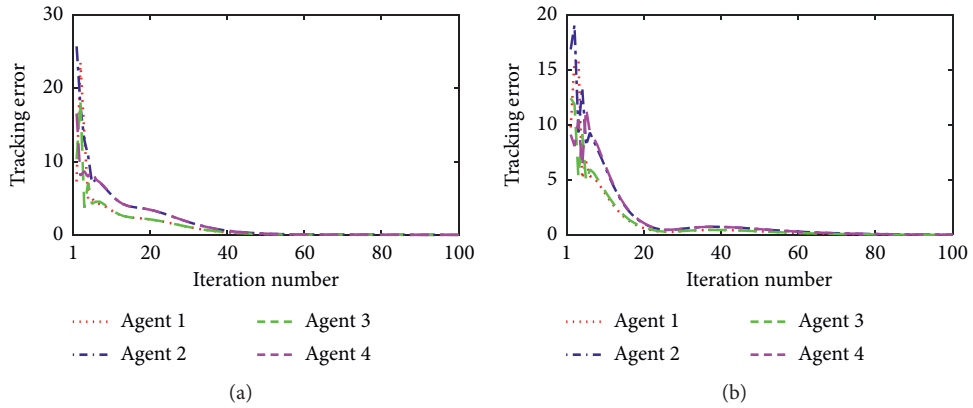

Figure 4: The 2-norm of tracking errors for all agents in each interaction by open-loop PD$^{\alpha}$-type. (a) Tracking errors of $y1$ with iterations. (b) Tracking errors of $y2$ with iterations.

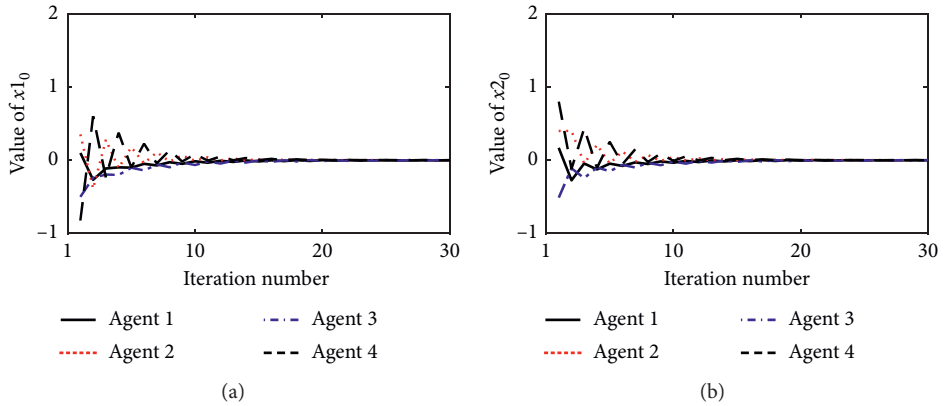

Figure 5: Initial state profile vs. iteration number by closed-loop PD$^{\alpha}$-type. (a) Initial state learning of $x1$. (b) Initial state learning of $x2$.

desired trajectory over the time period [0, 1]. We define the errors in the 2-norm sense at the ith iteration as $\|y_{d,1} - y1_{i,j}\|_2$ and $\|y_{d,2} - y2_{i,j}\|$ for $j = 1, 2, 3, 4$. Figure 4 depicts the tracking errors in each iteration; it shows that the tracking errors converge to zero as the iteration number increases. By the 60th iteration, the tracking errors of $y1$ of the four followers in the 2-norm sense are 0.000456, 0.000862, 0.000351, and 0.000785, respectively. By the 80th iteration, the tracking errors of $y2$ of the four followers in the 2-norm sense are 0.000648, 0.000978, 0.000596, and 0.000895, respectively.

Case 2. Closed-loop PDα-type: the initial inputs and initial state of the multiagents are the same as Case 1. Based on Theorem 2, we select the learning gains as $\Gamma_{P2} = \begin{bmatrix} 0.504 & 0 \\ 0 & 0.396 \end{bmatrix}$,$\Gamma_{D2} = \begin{bmatrix} 6 & 0 \\ 0 & 7 \end{bmatrix}$. Clearly, $\rho_2 = (1/\|\mathbf{I} + \mathbf{H} \otimes \Gamma_{D2}\mathbf{CB}\|) = 0.2146 < 1$; thus, the convergence condition can be satisfied.

Figures 5–7 show the trajectory tracking performances employing the closed-loop PD$^{\alpha}$-type ILC scheme. As it can be seen from Figure 5, similar to the simulation results of Case 1, the initial state of the agents tends to reach the desired initial state as the iteration number increases. Figure 6 shows the outputs $y1$ and $y2$ with closed-loop PD$^{\alpha}$-type ILC at the 5th and 30th iterations. From Figure 6, the trajectories $y1$ and $y2$ of the followers can track the desired trajectory generated by the leader as the iteration number increases over the time period [0, 1]. Figure 7 shows the tracking errors of $y1$ and $y2$ of the four followers in 2-norm sense with the number of iterations. It can be seen that the errors gradually decrease and approach zero as the number of iteration increases. By the 30th iteration, the tracking errors of $y1$ of the four followers in 2-norm sense are 0.000279, 0.000648, 0.000324, and 0.000472. The tracking errors of $y2$ of the four followers in 2-norm sense are, respectively, 0.000187, 0.000547, 0.000298, and 0.000385. Besides, compared with the open-loop PD$^{\alpha}$-type, the closed-loop FOILC performs better and has faster convergence speed than the open-loop one.

Case 3. Open-closed-loop PD$^{\alpha}$-type

In this simulation, the initial states and inputs are the same as Case 1 and Case 2. According to Theorem 3, the learning gain matrix can be obtained as follows:

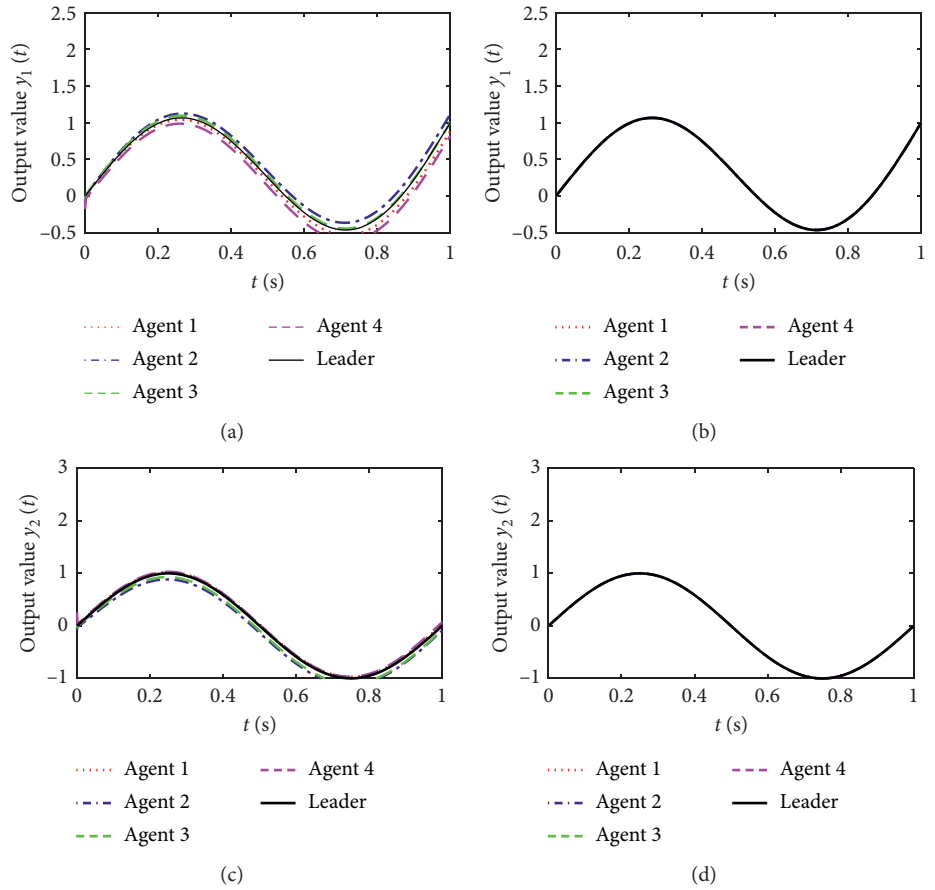

FIGURE 6: The tracking results of all agents at different iterations by closed-loop PD$^{\alpha}$-type. (a) Trajectories of $y1$ at the 5th iteration. (b) Trajectories of $y1$ at the 30th iteration. (c) Trajectories of $y2$ at the 5th iteration. (d) Trajectories of $y2$ at the 30th iteration.

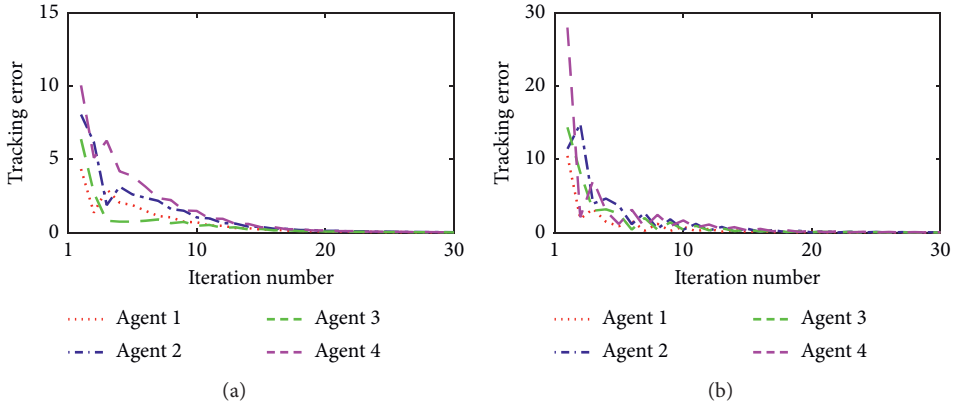

FIGURE 7: The 2-norm of tracking errors for all agents in each interaction by closed-loop PD$^{\alpha}$-type. (a) Tracking errors of $y1$ with iterations. (b) Tracking errors of $y2$ with iterations.

$$\Gamma_{P1} = \begin{bmatrix} 0.616 & 0 \\ 0 & 0.484 \end{bmatrix}, \quad \Gamma_{P2} = \begin{bmatrix} 0.5 & 0 \\ 0 & 0.4 \end{bmatrix},$$
$$\Gamma_{D1} = \begin{bmatrix} 4.5 & 0 \\ 0 & 1.8 \end{bmatrix}, \quad \Gamma_{D2} = \begin{bmatrix} 6 & 0 \\ 0 & 7 \end{bmatrix}. \tag{58}$$

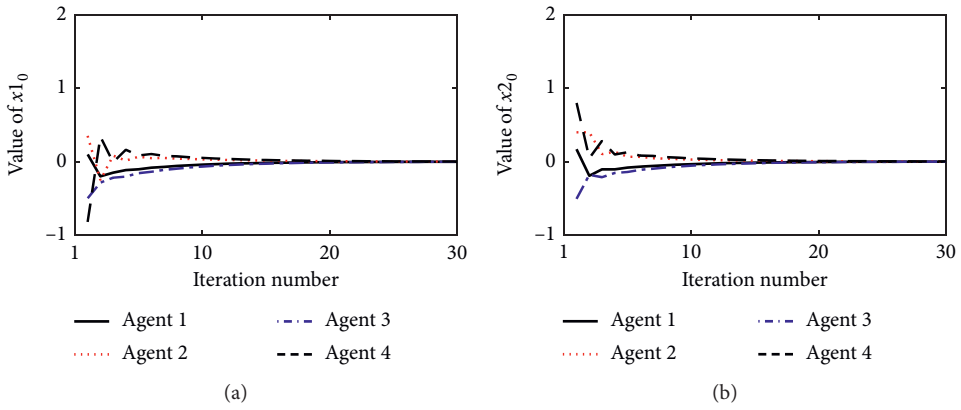

FIGURE 8: Initial state profile vs. iteration number by open-closed-loop PD$^{\alpha}$-type. (a) Initial state learning of $x1$. (b) Initial state learning of $x2$.

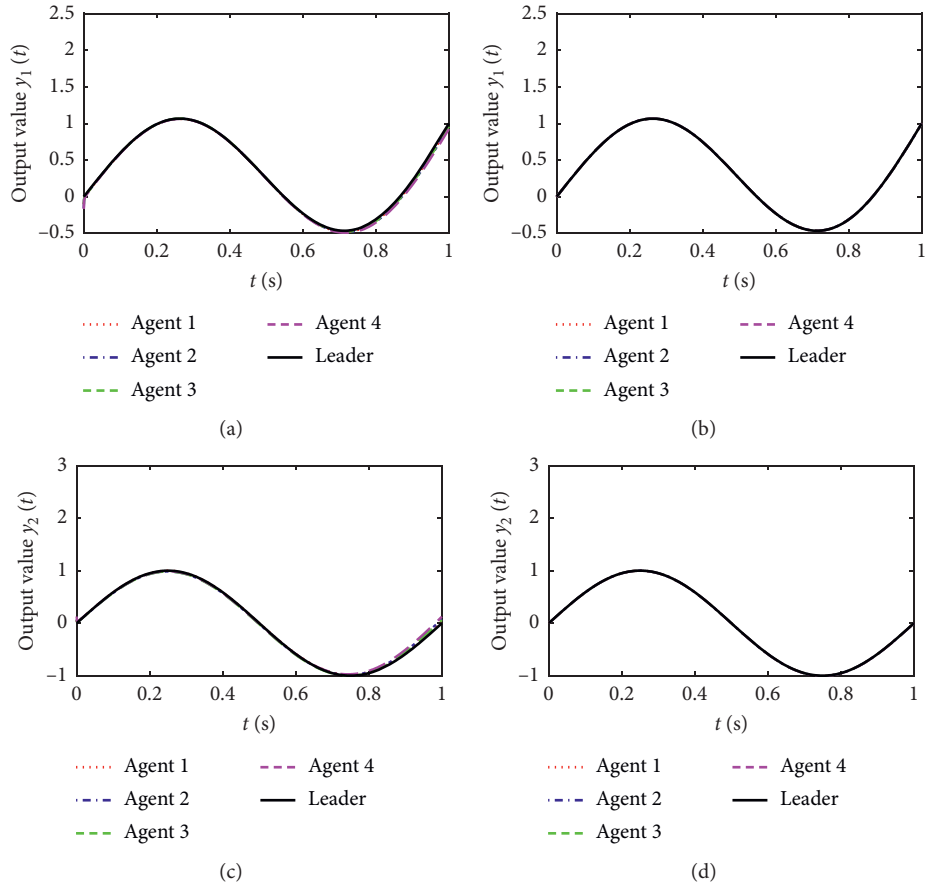

FIGURE 9: The tracking results of all agents at different iterations by open-closed-loop PD$^{\alpha}$-type. (a) Trajectories of $y1$ at the 5th iteration. (b) Trajectories of $y1$ at the 30th iteration. (c) Trajectories of $y2$ at the 5th iteration. (d) Trajectories of $y2$ at the 30th iteration.

Clearly, $\rho_2\rho_1 = 0.245 < 1$; thus, the convergence condition in Theorem 3 can be satisfied.

The simulation results with open-closed-loop PD$^{\alpha}$-type FOILC are presented in Figures 8–10. The results are similar to those of the open-loop and closed-loop PD$^{\alpha}$-type FOILC. From the results, both the initial states and the outputs can converge to the desired values. And we can conclude that the proposed FOILC scheme with initial state learning works well as the iteration number increases. Figure 9 shows the output tracking results of $y1$ and $y2$. It can be seen that the followers can fully track the desired trajectory as the iteration increases over the time

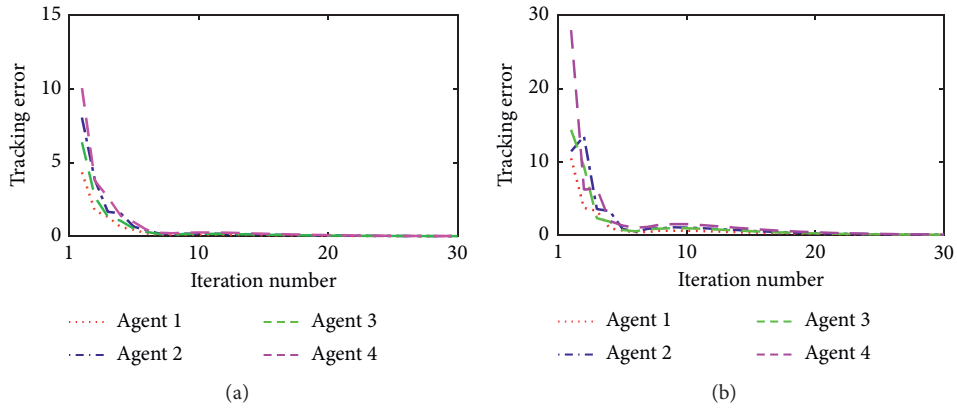

FIGURE 10: The 2-norm of tracking errors for all agents in each interaction by open-closed-loop PD$^{\alpha}$-type. (a) Tracking errors of $y1$ with iterations. (b) Tracking errors of $y2$ with iterations.

period [0, 1].In addition, compared with open-loop PD$^{\alpha}$-type FOILC and closed-loop PD$^{\alpha}$-type, applying open-closed-loop PD$^{\alpha}$-type FOILC has better performance in the initial state and for the outputs.

5. Conclusion

In this paper, we have discussed the consensus problem with fixed communication graph, which has been addressed for fractional-order multiagent systems with initial state shift. Considering the initial state learning mechanism, open-loop PD$^{\alpha}$ type, closed-loop PD$^{\alpha}$ type, and open-closed-loop PD$^{\alpha}$ type FOILC are proposed. The theoretical convergence of the proposed algorithm is analyzed and sufficient conditions are presented. Theoretical analysis shows that the proposed algorithms can guarantee the tracking errors of all the agents and the errors in the initial state tend to be zero in a finite time as the number of iterations increases. Finally, some simulation examples are used to validate the effectiveness. As a recommendation for the future, the convergence and robustness of fractional-order nonlinear systems can be studied by using the proposed method of this paper.

Data Availability

The data used to support the findings of this study are available from the corresponding author upon request.

Conflicts of Interest

The authors declare that there are no conflicts of interest regarding the publication of this paper.

Acknowledgments

This study has been supported by the National Natural Science Foundation of China (no. 61871163), the Zhejiang Provincial Natural Science Foundation of China (no. LQ19E070003), and Zhejiang Provincial Key Lab of Equipment Electronics.

References

[1] J. Fu, G. Wen, W. Yu, and Z. Ding, "Finite-time consensus for second-order multi-agent systems with input saturation," *IEEE Transactions on Circuits and Systems II: Express Briefs*, vol. 65, no. 11, pp. 1758–1762, 2018.

[2] Y. Cao, L. Zhang, C. Li, and M. Z. Q. Chen, "Observer-based consensus tracking of nonlinear agents in hybrid varying directed topology," *IEEE Transactions on Cybernetics*, vol. 47, no. 8, pp. 2212–2222, 2017.

[3] Y. Tang and P. Yi, "Distributed coordination for a class of non-linear multi-agent systems with regulation constraints," *IET Control Theory & Applications*, vol. 12, no. 1, pp. 1–9, 2017.

[4] X. Wang and G.-H. Yang, "Adaptive reliable coordination control for linear agent networks with intermittent communication constraints," *IEEE Transactions on Control of Network Systems*, vol. 5, no. 3, pp. 1120–1131, 2018.

[5] Y. Cao, Y. Li, W. Ren, and Y. Chen, "Distributed coordination of networked fractional-order systems," *IEEE Transactions on Systems, Man, and Cybernetics, Part B: Cybernetics*, vol. 40, no. 2, pp. 362–370, 2010.

[6] Y. Cao and W. Ren, "Distributed formation control for fractional-order systems: dynamic interaction and absolute/relative damping," *Systems & Control Letters*, vol. 59, no. 3-4, pp. 233–240, 2010.

[7] C. Song and J. Cao, "Consensus of fractional-order linear systems," in *Proceedings of the 2013 9th Asian Control Conference (ASCC)*, Istanbul, Turkey, June 2013.

[8] C. Song, J. Cao, and Y. Liu, "Robust consensus of fractional-order multi-agent systems with positive real uncertainty via second-order neighbors information," *Neurocomputing*, vol. 165, pp. 293–299, 2015.

[9] Z. Yu, H. Jiang, and C. Hu, "Leader-following consensus of fractional-order multi-agent systems under fixed topology," *Neurocomputing*, vol. 149, no. PB, pp. 613–620, 2015.

[10] Z. Yu, H. Jiang, C. Hu, and J. Yu, "Leader-following consensus of fractional-order multi-agent systems via adaptive pinning control," *International Journal of Control*, vol. 88, no. 9, pp. 1746–1756, 2015.

[11] Z. Yu, H. Jiang, C. Hu, and J. Yu, "Necessary and sufficient conditions for consensus of fractional-order multiagent systems via sampled-data control," *IEEE Transactions on Cybernetics*, vol. 47, no. 8, pp. 1892–1901, 2017.

[12] Z. Yaghoubi and H. A. Talebi, "Cluster consensus of general fractional-order nonlinear multi agent systems via adaptive

sliding mode controller," *Archives of Control Sciences*, vol. 29, no. 4, pp. 643–665, 2019.

[13] F. Wang and Y. Yang, "On leaderless consensus of fractional-order nonlinear multi-agent systems via event-triggered control," *Nonlinear Analysis: Modelling and Control*, vol. 24, no. 3, pp. 353–367, 2019.

[14] D. Luo, J. Wang, and D. Shen, "P D α type distributed learning control for nonlinear fractional order multiagent systems," *Mathematical Methods in the Applied Sciences*, vol. 42, no. 13, pp. 4543–4553, 2019.

[15] Y. Li, Y. Chen, and H.-S. Ahn, "Fractional-order iterative learning control for fractional-order linear systems," *Asian Journal of Control*, vol. 13, no. 1, pp. 54–63, 2011.

[16] Y. Li, Y. Chen, H.-S. Ahn, and G. Tian, "A survey on fractional-order iterative learning control," *Journal of Optimization Theory and Applications*, vol. 156, no. 1, pp. 127–140, 2013.

[17] S. Lv, M. Pan, X. Li et al., "Consensus tracking of fractional-order multiagent systems via fractional-order iterative learning control," *Complexity*, vol. 2019, no. 8, 11 pages, Article ID 2192168, 2019.

[18] D. Luo, J. Wang, and D. Shen, "Learning formation control for fractional-order multiagent systems," *Mathematical Methods in the Applied Sciences*, vol. 41, no. 13, pp. 5003–5014, 2018.

[19] J. Wang, T. Yang, G. Staskevich et al., "Approximately adaptive neural cooperative control for nonlinear multiagent systems with performance guarantee," *International Journal of Systems Science*, vol. 48, no. 5-1, pp. 909–920, 2017.

[20] X. H. Bu, Z. S. Hou, and F. S. Yu, "Iterative learning control for a class of linear continuous-time switched systems," *Control Theory and Applications*, vol. 29, no. 8, pp. 1051–1056, 2012.

[21] A. A. Kilbas, H. M. Srivastava, and J. J. Trujillo, *Theory and Applications of Fractional Differential Equations*, Elsevier, Amsterdam, The Netherlands, 2006.

[22] S. Westerlund and L. Ekstam, "Capacitor theory," *IEEE Transactions on Dielectrics and Electrical Insulation*, vol. 1, no. 5, pp. 826–839, 1994.

[23] I. Podlubny, *Fractional Differential Equations*, Academic Press, Cambridge, MA, USA, 1999.